SAND2020-2036C

Wind turbine aerodynamic measurements using a scanning lidar

C L Kelley[1], T G Herges[1], P Doubrawa[2], L A Martinez[2] and T Mikkelsen[3]

[1]Sandia National Laboratories, Wind Energy Technologies, Albuquerque, NM, USA.
[2]National Renewable Energy Laboratory, National Wind Technology Center, Boulder, CO, USA.
[3]Technical University of Denmark, Department of Wind Energy, Roskilde, Denmark.

E-mail: clkell@sandia.gov

Abstract. A method for measuring wake and aerodynamic properties of a wind turbine with reduced error based on simulated lidar measurements is proposed. A scanning lidar measures airspeed projected onto its line-of-sight. However, line-of-sight is rarely parallel to the velocities of interest. The proposed line-of-sight projection correction technique showed reduced axial velocity error for a simple wake model. Next, an analysis based on large-eddy simulations of a V27 wind turbine was used to more accurately assess the projection correction technique. During the simulation, flow behind the turbine is sampled with a virtual lidar matching the scanning geometry and sampling frequency of the DTU SpinnerLidar. The axial velocity, axial induction, freestream wind speed, thrust coefficients, and power coefficients are calculated from virtual lidar measurements using two different estimates of the flow: line-of-sight velocity without correction, and line-of-sight with projection correction. Results indicate that all wake and aerodynamic quantity error is reduced significantly by using the projection correction technique. Axial velocity error is reduced on average from 7.4% to 2.8%.

1. Introduction

A scanning lidar, with sufficient spatial and temporal resolution, allows for unique experiments on wind turbines and studies of the complex flow field downstream of a wind turbine in its wake. One such instrument is the SpinnerLidar designed by the Technical University of Denmark [1] and recently deployed in a test campaign at Sandia's Scaled Wind Farm Technology (SWiFT) site [2, 3]. The experiment was focused on wind turbine wakes [4], the efficacy of wake steering through intentional yaw [5], and the impact of these steered wakes on plant energy capture and unsteady loads. This paper is focused on how to best derive aerodynamic quantities from these scanning lidar measurements. This makes it possible to measure integral aerodynamic performance (for example thrust and power coefficient) without the need for an instrumented blade. There are complicating issues in this analysis: the lidar measurement is the projection of the actual velocity in the line-of-sight direction (LOS), and the probe volume averages this velocity projection in space. All of these issues introduce error to the wake and aerodynamic quantities being derived.

The line-of-sight projection correction technique is first evaluated with a simple wake model in section 2. Next, a more realistic wake simulation of a V27 is used to further test the lidar

correction for a realistic, turbulent flow field. The simulation parameters are summarized in section 3. These simulations allowed the exact wake and aerodynamic quantities (no spatial averaging or projection error) to be compared to the virtual lidar measurements, and the associated errors to be quantified. Section 4 focuses on axial velocity, section 5 on measuring freestream wind speed, and section 6 discusses aerodynamic properties such as induction, thrust, and power in the wake as estimated by a virtual scanning lidar.

2. Line-of-Sight Projection Correction

The velocity measured by a lidar is the actual velocity projected onto the line-of-sight direction. If α is the angle between these two directions, then from the definition of the vector dot-product it is known that

$$|\mathbf{V}_{LOS}| = |\mathbf{V}| \cos(\alpha). \tag{1}$$

Schmidt et. al used the line-of-sight projection correction approach, dividing by the cosine of the subtended angle, to solve for wind direction offset for aligning a lidar with sonic anemometers [6].

If it is assumed that perfect knowledge of wind direction is known everywhere, or on average the wind direction is parallel everywhere, then α is known, and the actual wind magnitude can be solved for, $V_{LOSPC} = \frac{V_{LOS}}{\cos(\alpha)}$. Throughout this paper this method will be referred to as line-of-sight projection correction (LOSPC). Also, the average wind direction is known in this paper from the simulations to be parallel with the axis of rotation. If applied to an experiment, the average wind direction would need to be measured. The LOSPC method can only be applied after probe volume spatial averaging takes place. So there will always be error that cannot be corrected due to probe volume spatial averaging.

Figure 1a estimates this error for a simple wake model with LOSPC. The velocity field is 1 outside the wake, and $\frac{2}{3}$ inside the wake. Rays emanating from the lidar source had spatial averaging applied and the axial velocity error was found. The maximum error occurs at the edge of the wake where the velocity field changes rapidly and spatial averaging most affects the measurement. The velocity error on the black arc with a focal distance of $3D$ is shown in figure 1b. The lidar overestimates the velocity magnitude inside the wake edge (as much as 24%) and underestimates the velocity outside the wake edge (as much as 18%). In addition, it can be seen that a velocity measurement using a lidar near a high gradient has higher error. The LOSPC showed significant improvement in axial velocity error, especially near the periphery of the field-of-view (FOV).

Forsting et. al modeled the error associated with the volumetric averaging of measuring the wake flow field behind a wind turbine [7]. Their results showed that a lidar underpredicts velocity outside the wake edge, and overpredicts velocity inside the wake edge by approximately 25–30% for a pulsed lidar due to volumetric averaging, which agrees well with this simple wake model.

3. Simulation parameters for virtual lidar testing

A simulation of the V27 wind turbine was performed in SOWFA with stable atmospheric conditions by Churchfield [8]. SOWFA implements the actuator line representation of the rotor, which uses a FAST model of the V27 for lift and drag forces. This simulation used a uniform 10 m resolution grid that is 3 km in each direction along the ground, and 1 km vertically. The time-step was 0.02 s. The hub height average wind speed was 6.5 m/s, the turbulence intensity was 8.5%, and the shear exponent was 0.29. These are representative inflow conditions for the Sandia SWiFT facility in Lubbock Texas [9]. The wind turbine had no average yaw; therefore the wake appears in the center of the field of view for the analyzed conditions. The simulation data analyzed lasted 200 seconds or 100 wake scans.

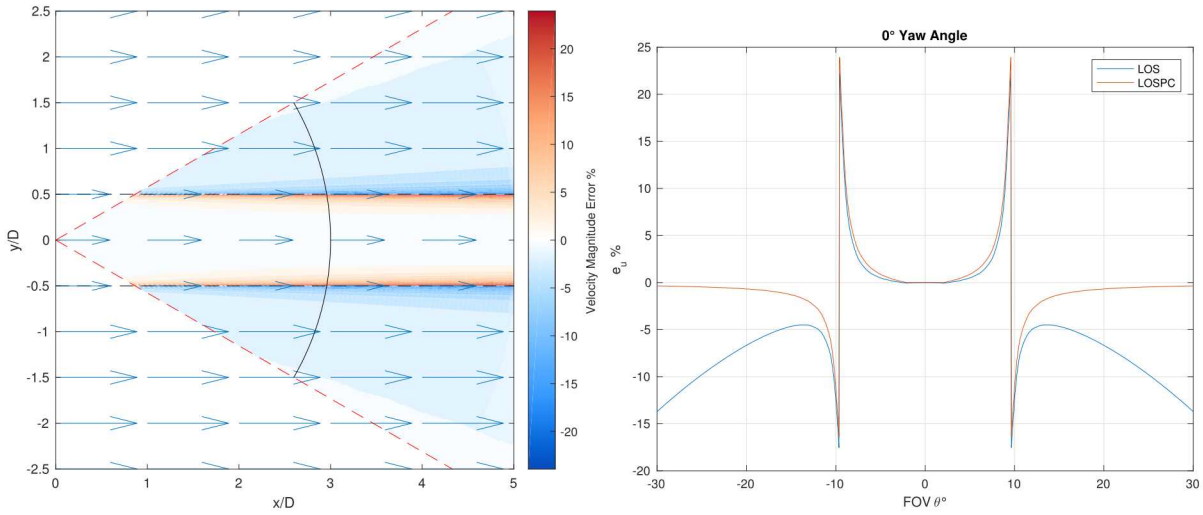

Figure 1. Simple wake model for LOSPC error of axial velocity due to probe volume averaging a) contour b) at a focal length of 3D.

4. Axial velocity estimation from virtual lidar measurements

The axial velocity was found with a virtual lidar sampling of the SOWFA simulation solution at a focal distance of $3D$ (81 m) downstream of the rotor plane. On this surface the exact axial velocity (u_{ex}), the line-of-sight velocity (u_{LOS}), and the line-of-sight velocity with projection correction (u_{LOSPC}) were found and can be seen in figure 2 for one lidar scan. u_{LOS} is found by equating axial velocity with the lidar line-of-sight measurement including spatial averaging. u_{LOSPC} is found by applying the projection correction to u_{LOS}. Axial velocity refers to the velocity component parallel to the wind turbine nacelle.

The wake edge and center are defined by a modified version of the wake tracking algorithm developed by Herges [10] that forces the area of the wake to be twice the area of the rotor disc. Actuator disc theory shows that the far-wake area is twice the rotor disc area if static pressure has returned to freestream static pressure, a reasonable assumption for wake measurements beyond $3D$ downstream [11]. The black line and center dot indicate the wake edge and wake center in figure 2.

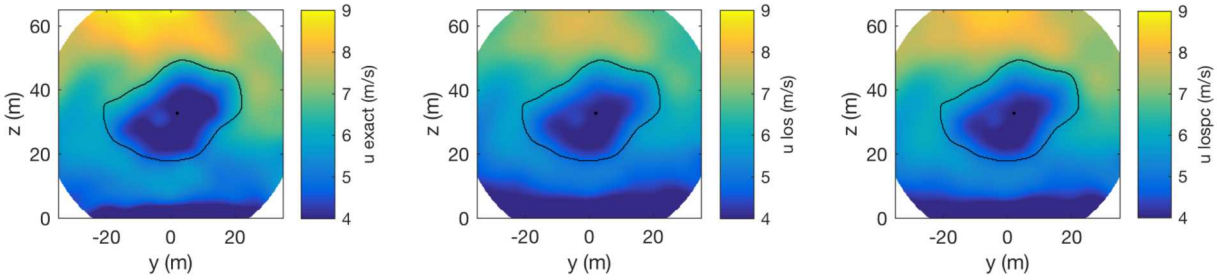

Figure 2. Axial velocity field a) exact, b) line-of-sight, and c) line-of-sight projection correction for one lidar scan.

The differences in the velocity field are subtle, so the error of axial velocity was found as the difference between each lidar measurement and the exact axial velocity field

$$e_{u_{LOS}} = \frac{u_{LOS} - u_{ex}}{u_{ex}} \tag{2}$$

and

$$e_{u_{LOSPC}} = \frac{u_{LOSPC} - u_{ex}}{u_{ex}}. \tag{3}$$

Figure 3a shows the axial velocity error spatially during one lidar scan (approximately 2 seconds). In general, the wake velocity is overpredicted towards the center of the wake, and underpredicted outside the wake. To improve upon the axial velocity measurement by the lidar, the line-of-sight projection correction technique (LOSPC) was applied and is plotted in figure 3b. Outside the wake, and towards the periphery of the FOV, the error is brought closer to zero, indicated by a greater area of white.

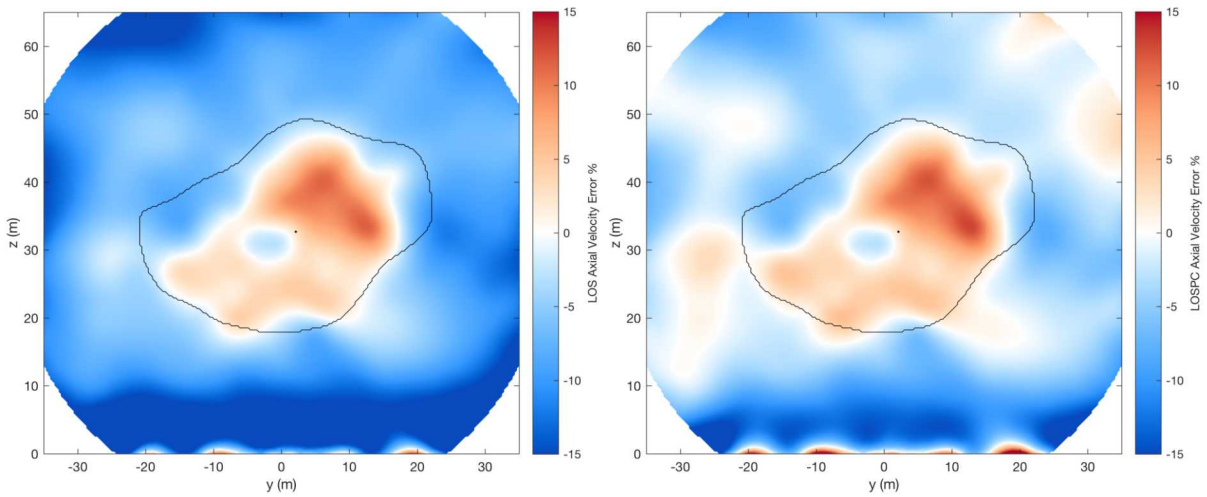

Figure 3. Axial velocity error from a) LOS and b) LOSPC.

A total of 100 lidar scans for a time evolving wake were collected from the simulation. The error associated with the LOS axial velocity and LOSPC axial velocity for the entire field of view and all scans were aggregated into probability density functions. Figure 4a shows that inside the wake, LOSPC improves axial velocity error minimally. Outside the wake, figure 4b shows that the LOSPC is useful in improving the error on average, and reducing the standard deviation of the error. Over the entire FOV for all 100 lidar scans, LOS axial velocity has an error of -7.4% and the LOSPC axial velocity has an error of -2.8%.

5. Freestream wind speed estimation from virtual lidar measurements

By averaging the velocity field across horizontal slices and by limiting the data points to those outside the wake, the boundary layer profile was measured using the scanning lidar. Figure 5 shows an instantaneous wind speed field with the wake ignored. The horizontal black line corresponds to the V27 hub height, 32.1 m. The projection correction technique reduces the error to give a more accurate prediction of the freestream velocity.

The average error of freestream velocity using the LOS measurement was 9.2% below the actual freestream velocity. Using the LOSPC approach the freestream velocity error was brought closer to zero, 3.5% below the exact freestream velocity. Freestream velocity at hub height is a necessary quantity to calculate induction, thrust coefficient, and power coefficient. A meteorological tower could measure hub height wind speed more accurately, however it is not located where the lidar measurement is taking place. Therefore, the freestream velocity measured with the lidar gives an instantaneous value at the lidar measurement plane.

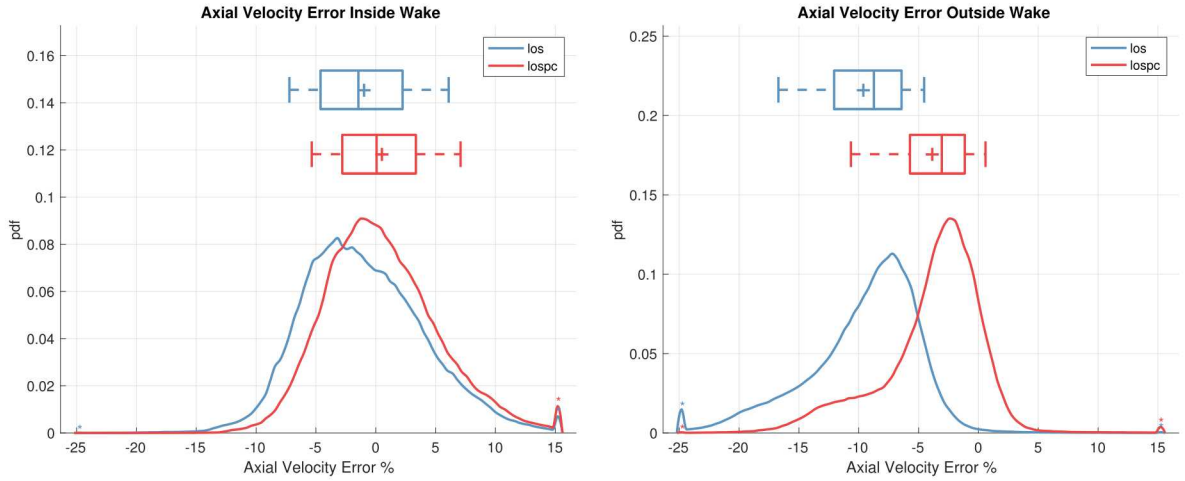

Figure 4. Distribution of axial velocity error at $3D$ for 100 lidar scans a) inside the wake b) outside the wake.

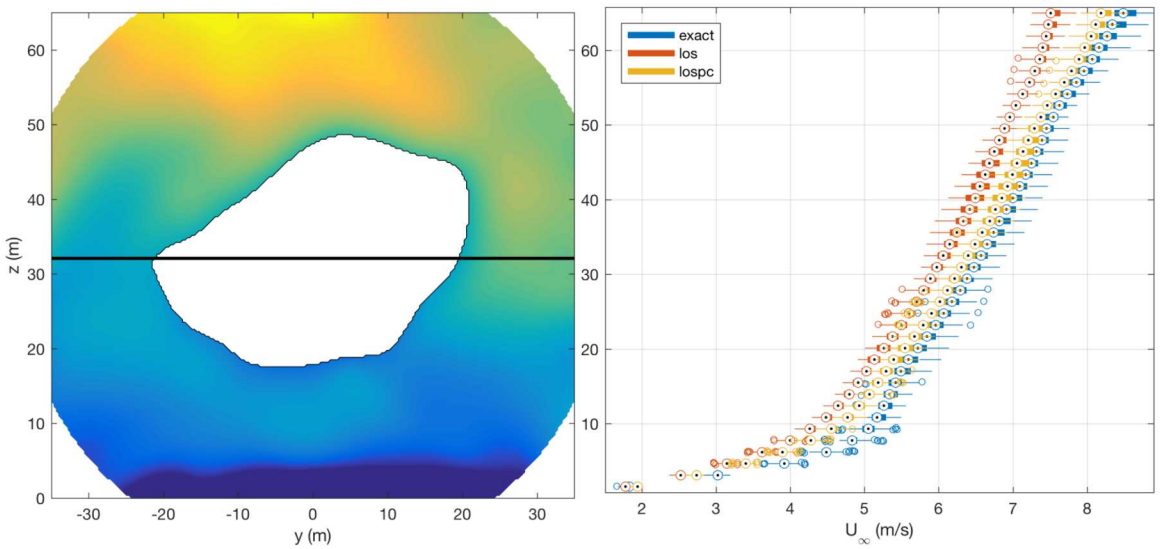

Figure 5. Atmospheric boundary layer from 100 lidar scans values lying on the same horizontal outside of wake.

6. Aerodynamic estimation from virtual lidar measurements

The lidar measurements at a focal distance of $3D$ were used to investigate axial induction, thrust coefficient, and power coefficient.

6.1. Azimuthal average wake induction

In blade element momentum theory, the axial induction is representative of how much the axial velocity is slowed down by an infinite number of slender blades at the rotor disc, and the axial induction is constant in the azimuthal direction. This theory inspired the following approach whereby the wake may distort and expand in shape from a perfect circle to a more generic shape, as identified by the wake tracking algorithm, and the average induction on each annulus was found.

To find the azimuthal average induction, contours are overlaid on the lidar scan of the wake

from the center to the edge to define the distorted annuli seen in figure 6. The wake edge and center are defined by a modified version of the wake tracking algorithm developed by Herges [10] that forces the area of the wake to be twice the area of the rotor disc. Actuator disc theory shows that the far-wake area is twice the rotor disc area if static pressure has returned to freestream static pressure, a reasonable assumption for wake measurements beyond $3D$ downstream [11].

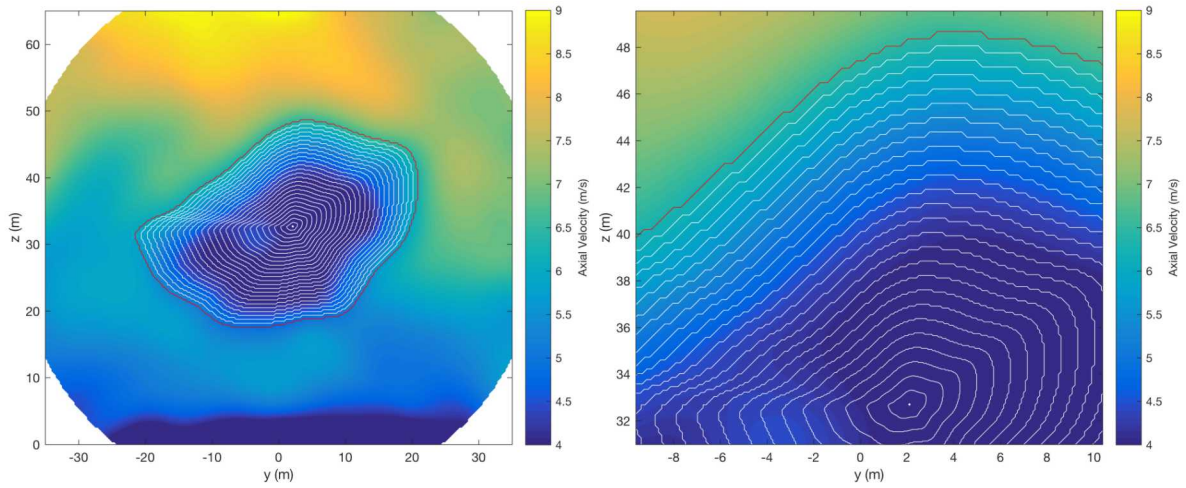

Figure 6. Distorted wake shape annuli and zoomed view.

On each distorted annulus, the average induction was found

$$\overline{a} = \frac{1}{2\pi} \int_0^{2\pi} \left(1 - \frac{u_{wake}}{U_\infty}\right) \mathrm{d}\theta. \tag{4}$$

Figure 7 shows the results of calculating wake induction, $\overline{a}$, for each distorted annulus, where $\frac{r}{R}$ is the normalized distance from the wake center ($\frac{r}{R}$=0) to the wake edge ($\frac{r}{R}$=1). The wake shows a bell-curve shaped velocity profile, and the error bars correspond to $\pm\sigma(\overline{a})$ of the 100 lidar scans. Consistent with figure 3, the LOS and LOSPC lidar measurement introduces spatial averaging error inside the wake that overpredicts axial velocity, therefore the axial induction is seen here to be underpredicted. Because the induction relies on knowing the freestream velocity, LOSPC is advantageous for reducing error of induction even inside the wake.

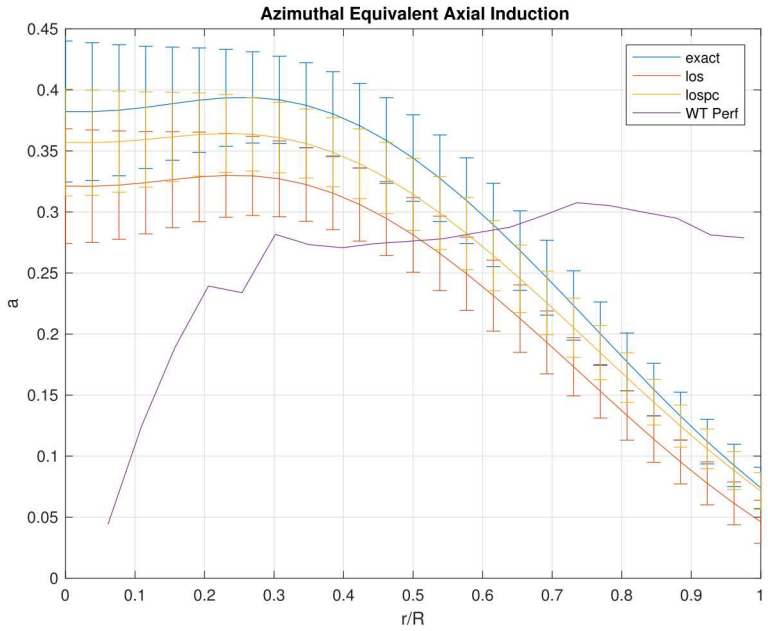

Figure 7. Wake, azimuthal average induction for 100 lidar scans.

Figure 7 also shows the axial induction at the rotor plane modeled with blade element momentum theory code, WT_Perf. The effect of nacelle drag and streamtube mixing mean that the radial induction profile in the wake does not match the blade loading at the rotor disc. Therefore one cannot equate mass flow from each distorted wake annulus to the rotor disc annulus to solve for the rotor disc induction. However, if the focal length of the lidar was reduced from $3D$ to closer to the rotor disc, it may be possible to measure the blade load distribution in the wake.

6.2. Thrust coefficient

The thrust coefficient describes the momentum deficit in the wake. If the deficit is measured in the far-wake, when pressure has recovered, the momentum deficit is also equal to the thrust on the rotor. A derivation of thrust for a wind turbine wake control volume is presented in Frandsen [11]. The thrust coefficient was found for 100 lidar scans of the simulation at a focal length of $3D$. The freestream velocity was found from a horizontal slice at hub height for each frame. The axial velocity, $u(z, y)$, was taken from the virtual lidar measurements, and the various correction methods were applied. The thrust coefficient is provided in terms of wake velocity. The thrust force found by integrating the momentum deficit at the actuator disc is half the thrust found by integrating the momentum deficit in the far wake because the static pressure at the rotor disc is not freestream static pressure.

$$C_{T_{wake}} = \frac{2}{\pi R^2} \iint\limits_{wake} \frac{u(z,y)}{U_\infty} \left(1 - \frac{u(z,y)}{U_\infty}\right) \mathrm{d}z\, \mathrm{d}y \tag{5}$$

Figure 8 shows the distribution of thrust coefficient calculated from the entire FOV for 100 lidar scans. The LOSPC is beneficial because the mean value of thrust is closer the exact value, and the spread of thrust for the various scans is reduced. The average thrust coefficient error is improved from -15.1% to -4.6%.

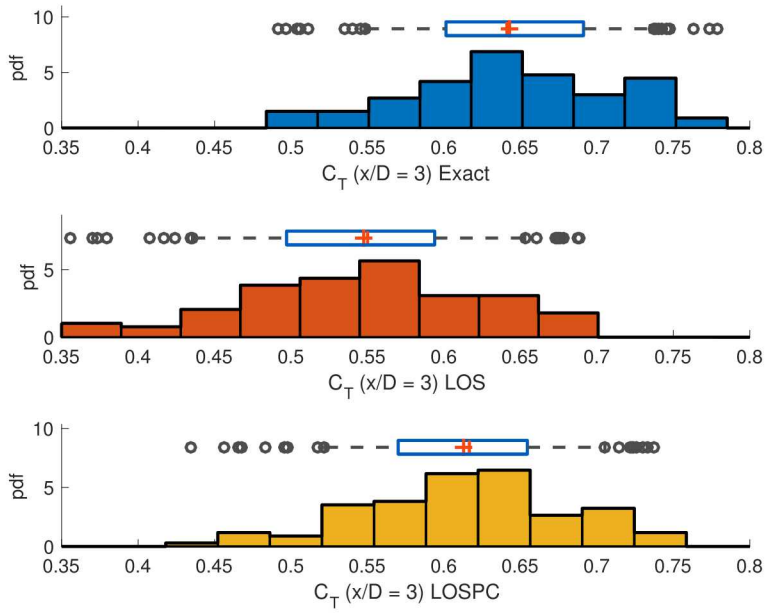

Figure 8. Distribution of thrust coefficient from 100 lidar scans at $f = 3D$.

6.3. Power coefficient

Just as with the thrust coefficient, power coefficient can also be measured from the wake assuming no mixing of the freestream into the wake.

$$C_{P_{wake}} = \frac{1}{\pi R^2} \iint\limits_{wake} \frac{u(z,y)}{U_\infty} \left(1 - \frac{u^2(z,y)}{U_\infty^2}\right) \mathrm{d}z\,\mathrm{d}y \tag{6}$$

The power coefficient was found for the same 100 lidar scans of the wake and can be seen in figure 9. Again, the LOSPC brings the calculated power coefficient closer to the exact value improving error from -13.2% to -3.5%.

To improve the prediction of wind turbine aerodynamics using the lidar, it may be necessary to improve the wake edge detection algorithm, so one does not assume the wake area is twice to rotor disc area. Additionally, thrust and power coefficients presented here were calculated based on steady flow, axial flow. If the lidar could be used to track turbulence in addition to velocity, the thrust and power coefficient calculations could be refined to include momentum due to turbulence [11] by subtraction of unsteady terms.

$$C_{T_{wake}} = \frac{2}{\pi R^2} \iint\limits_{wake} \frac{u(z,y)}{U_\infty} \left(1 - \frac{u(z,y)}{U_\infty}\right) - \frac{2}{\pi R^2} \iint\limits_{wake} TI^2(z,y)\,\mathrm{d}z\,\mathrm{d}y \tag{7}$$

$$C_{P_{wake}} = \frac{1}{\pi R^2} \iint\limits_{wake} \frac{u(z,y)}{U_\infty} \left(1 - \frac{u^2(z,y)}{U_\infty^2}\right) \mathrm{d}z\,\mathrm{d}y - \frac{1}{\pi R^2} \iint\limits_{wake} \frac{5u(z,y)}{U_\infty} TI^2(z,y)\,\mathrm{d}z\,\mathrm{d}y \tag{8}$$

7. Conclusions

A simple wake model with a top-hat profile showed that a lidar has the greatest amount of error due to spatial averaging where the velocity field has the largest gradient. In addition, the

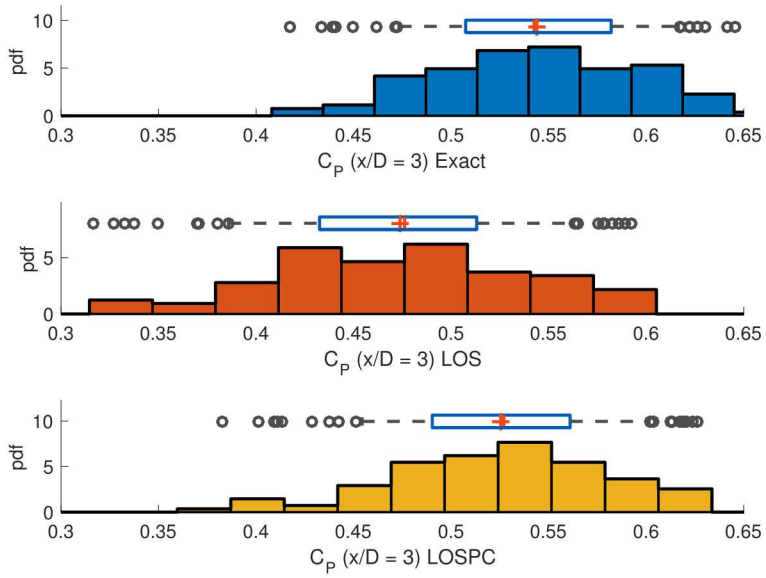

Figure 9. Distribution of power coefficient from 100 lidar scans at $f = 3D$.

simple wake model motivated further evaluation of the LOSPC technique to correct LOS lidar measurements.

To further investigate the LOSPC technique in more realistic conditions, a SOWFA simulation with a virtual DTU SpinnerLidar was used to investigate error correction on wake and aerodynamic parameters. All parameters were calculated from the virtual lidar measurements. Table 1 summarizes the improvement in error. LOSPC is advantageous to use for all calculated wake and aerodynamic properties. In addition, as seen in figure 3, the spatial error in a single scan is also reduced.

In this table, u is the average axial velocity over the entire field of view, $\overline{a}$ is the average induction for all annuli in the wake, U_∞ is the average wind speed for all heights, C_T and C_P are the average thrust and power coefficients, and all quantities are averaged for 100 lidar scans of the wake. Due to the universal improvement of error, the LOSPC is recommended to be applied for all calculated wake and aerodynamic quantities calculated from wake lidar measurements.

Table 1. Summary of Error for Average Values of 100 Lidar Scans.

Method	u (m/s)	u_{error}	$\overline{a}$	$\overline{a}_{error}$	U_∞ (m/s)	$U_{\infty_{error}}$	C_T	$C_{T_{error}}$	C_P	$C_{P_{error}}$
Exact	6.0	—	0.29	—	6.5	—	0.64	—	0.54	—
LOS	5.6	-7.4%	0.24	-18.7%	5.9	-9.2%	0.55	-15.1%	0.47	-13.2%
LOSPC	5.9	-2.8%	0.27	-7.6%	6.2	-3.5%	0.61	-4.6%	0.53	-3.5%

The projection corrected axial velocity measurements are consistently 2.8% underpredicted, meaning that the spatial averaging is the cause of this remaining error. An additional correction to axial velocity could be made such that $u_{final} = 1.028 u_{LOSPC}$ and should be investigated further.

There are a few areas where the current work could be improved and are promising areas of future work. A tool that could be used to improve the lidar measurements would be a post-processing step of using the DTU linearized flow model LINCOM [1]. This would provide

an alternative approach for correcting the LOS lidar measurement to wake and aerodynamic quantities. Also previously mentioned, a new wake tracking algorithm could be developed that does not rely on the wake area being twice the rotor disc area. Also, if the lidar focal length is be reduced, the induction closer to the rotor disc could be measured before mixing across the wake occurs which may be a way of measuring spanwise blade loading with a scanning lidar. Finally, thrust and power coefficient could be refined to include momentum due to turbulence if the lidar could measure turbulence intensity.

8. Acknowledgments

The authors would like to thank Matthew Churchfield for providing SOWFA simulations of the V27 wind turbine. The work described in this paper was supported by funding from the DOE Energy Efficiency and Renewable Energys Wind Energy Atmosphere to Electrons (A2e) Program.

References

[1] Mikkelsen T, Astrup P and van Dooren M F The lidar cyclops syndrome bypassed: 3d wind field measurements from a turbine mounted lidar in combination with a fast cfd solver

[2] Mikkelsen T K, Herges T, Astrup P, Sjöholm M and Naughton B 2017 Wind field re-construction of 3d wake measurements from a turbine-installed scanning lidar *International Conference on Future Technologies for Wind Energy WindTech 2017 24-26 Oct. 2017*

[3] Naughton B, Schreck S and Wright A A2e wake steering experiment URL `https://a2e.energy.gov/projects/wake`

[4] Fleming P, Churchfield M, Scholbrock A, Clifton A, Schreck S, Johnson K, Wright A, Gebraad P, Annoni J, Naughton B, Berg J, Herges T, White J, Mikkelsen T, Sjholm M and Angelou N 2016 *Journal of Physics: Conference Series* **753** 052003

[5] Gebraad P, Thomas J J, Ning A, Fleming P and Dykes K 2017 *Wind Energy* **20** 97–107

[6] Schmidt M, Trujillo J J and Khn M 2016 *Journal of Physics: Conference Series* **749** 012005

[7] Forsting A R M, Troldborg N and Borraccino A 2017 *Journal of Physics: Conference Series* **854** 012014

[8] Churchfield M, Wang Q, Scholbrock A, Herges T, Mikkelsen T and Sjholm M 2016 *Journal of Physics: Conference Series* **753** 032009 URL `http://stacks.iop.org/1742-6596/753/i=3/a=032009`

[9] Kelley C L and Ennis B L *SAND Resport*

[10] Herges T G, Maniaci D C, Naughton B T, Mikkelsen T and Sjholm M 2017 *Journal of Physics: Conference Series* **854** 012021

[11] Frandsen S T *et al.* 2007 *Turbulence and turbulence-generated structural loading in wind turbine clusters*